https://doi.org/10.17113/ftb.63.04.25.8666 original scientific paper

Effect of Apigenin-Enriched *Elsholtzia splendens* Flower Extract on Lipid and Reactive Oxygen Species (ROS) Accumulation in 3T3-L1 Cells and *Caenorhabditis elegans*

Running head: *E. splendens* Inhibits Lipid Accumulation in 3T3-L1 Cells and *C. elegans*

Seulbi Lee[1], Soo-Im Choi[2] and Miran Jang[1,3*]

[1]Department of Smart Food & drug, Inje University, 197, Inje-ro, Gimhae-si, Gyeongsangnam-do, Republic of Korea
[2]MEDIOGEN Co., Ltd. R&D Center, 120, Bio Valley 1-ro, Jecheon-si, Chungcheongbuk-do, Republic of Korea
[3]Department of Food Technology and Nutrition, Inje University, 197, Inje-ro, Gimhae-si, Gyeongsangnam-do, Republic of Korea

Received: 11 April 2024
Accepted: 21 July 2025

SUMMARY

Research background. In the case of obesity, enlarged adipocytes cause lipid metabolism imbalance and increased oxidative stress, leading to excessive reactive oxygen species (ROS) production. ROS contributes to metabolic disorders such as inflammation and insulin resistance, further worsening lipid imbalance and promoting obesity-related diseases. Therefore, we investigated the benefits of *Elsholtzia splendens* that simultaneously suppresses lipid accumulation and ROS.

Experimental approach. We determined the total flavonoid content of the extracts and analysed them by HPLC to identify the functional ingredients. Cell viability and proliferation were evaluated in 3T3-L1 cells. The total lipid and triglyceride (TG) contents of cells and nematodes were measured by Oil Red O and TG assay, respectively. A qPCR analysis was performed to investigate the mRNA and accumulated ROS in nematodes.

*Corresponding author:
Phone: +82553203234
E-mail: mrjang@inje.ac.kr

Results and conclusions. Apigenin was the major substance in the *E. splendens* extracts and was most abundant in the flower part. The *E. splendens* flower extract (ESFE) did not show toxicity at concentrations of 25–100 μg/mL and had the highest apigenin content, thus we used ESFE in the subsequent test. ESFE and apigenin inhibited total lipid and TG accumulation in 3T3-L1 cells and nematodes. These effects were attributed to the inhibition of PPARγ and C/EBPα expression, factors involved in adipocyte differentiation. In addition, ESFE and apigenin induced the nuclear localization of DAF-16, which is involved in lipogenesis in nematodes. Also, ESFE and apigenin inhibited ROS accumulation in nematodes.

Novelty and scientific contribution. Research on *E. splendens* has mainly focused on its cultivation and growth. Research on the effects of *E. splendens* on metabolic diseases, including obesity, has been limited and this study provides new insights. Our results imply that ESFE is a valuable material to inhibit lipid and ROS accumulation, and suggest that apigenin-rich functional plant materials should be considered as potential agents against obesity and related diseases.

Keywords: *Elsholtzia splendens*; apigenin; lipid accumulation; reactive oxygen species (ROS); 3T3-L1 cells; *Caenorhabditis elegans*

INTRODUCTION

Obesity can be defined as an increase in body size and weight due to the excessive accumulation of lipids, and not only affects body shape but also causes chronic metabolic diseases such as type 2 diabetes, hyperlipidaemia, arteriosclerosis, and cardiovascular disease (*1*). Therefore, the seriousness of obesity is indisputable. The best of the various therapeutic solutions involves the suppression of fat accumulation in the body (*1,2*). Many gene products, including fatty acid synthase, fatty acid-binding protein, glucose transporter 4, and apolipoprotein, are involved in fat deposition during adipogenesis (*3,4*). Significantly, peroxisome proliferator-activated receptor γ (PPARγ) contributes to the maturation of adipocytes and lipid accumulation in cooperation with CCAAT/enhancer-binding protein α (C/EBPα) (*4*). Studies on substances that suppress lipid accumulation by controlling the expressions of PPARγ and C/EBPα continue (*5*).

Studies using Caenorhabditis elegans are conducted via high-throughput screening (HTS), which can bridge the gap between *in vitro* and *in vivo* mammalian model studies (*6,7*). DAF-16 is the only homolog of the forkhead box O (FOXO) family of transcription factors in *C. elegans* (*8*). DAF-16/FOXO is associated with insulin resistance and participates in processes of apoptosis, cell cycle regulation, stress resistance, and energy metabolism (*9,10*). In particular, FOXO1 is well known to be involved in the regulation of the cell cycle during differentiation (*9-11*). Many studies have

demonstrated that PPARγ is a prerequisite for adipocyte differentiation and that activated FOXO1 regulates PPARγ to inhibit adipogenesis (*9-11*). In addition, DAF-16/FOXO is closely related to resistance to oxidative stress and thus influences reactive oxygen species (ROS) generation (*12*).

Metabolic disorders with obesity commonly cause excessive ROS accumulation and can be fatal (*2*). Various studies have demonstrated that imbalanced lipid metabolism in obesity causes metabolic stress and increases ROS production in the body (*13*). In particular, high-sugar diets accelerate oxidative stress, which is defined as glucose toxicity with hyperglycemia (*14*). Therefore, to prevent chronic metabolic disorders, there is a need to identify a material that has significant antioxidant activity and suppresses lipid accumulation (*15,16*).

Elsholtzia splendens is a perennial herb belonging to the Lamiaceae family and has been used in traditional medicine. It is used as an ingredient in folk medicines to treat coughs, pain, and inflammation in North-East Asia (*17*). The plant is aromatic and has been reported to contain essential oils and compounds, such as elsholtzia ketone, naginata ketone, isobutyl isovalerate, geraniol, and geranyl acetate (*18,19*), and its phenolic contents include hesperidin, rutin, luteolin, quercetin, and apigenin (*20-22*). Furthermore, the phenolics in *E. splendens* extracts have been reported to have positive effects on aging through ROS inhibition, regulate microbial and viral growth, improve blood lipid levels, reduce inflammation, and have beneficial effects on Alzheimer's disease (*20,22-24*). In particular, a previous study reported that *E. splendens* collected from various plant regions commonly contain apigenin (*21*). Various plants containing apigenin and apigenin glycosides have antitumor and hepatoprotective effects and positively influence the cardiovascular and nervous systems (*25-27*). In addition, many studies have reported that apigenin regulates lipid metabolism (*26-28*).

This study investigated the total flavonoid and apigenin content of four parts of the plant (root, stem, leaf, and flower). Total lipid and triglyceride (TG) contents were measured in 3T3-L1 cells and *C. elegans* treated with *E. splendens* flower extract (ESFE), which has the highest flavonoid and apigenin content, to evaluate the inhibitory effect on lipid and ROS accumulation of ESFE. We also investigated the alterations in molecular factors involved in fat deposition in cells and nematodes to understand the mechanisms involved in the lipid accumulation inhibitory effect of ESFE.

MATERIALS AND METHODS

Reagents

Dulbecco's modified Eagle's minimum essential medium (DMEM), fetal bovine serum (FBS), trypsin-EDTA solution, phosphate buffered saline (PBS), penicillin-streptomycin, and normal goat serum (NGS) were obtained from WellGENE Biopharmaceuticals (Daegu, Korea). RNA extraction kits (Trizol reagent) were purchased from Invitrogen Corp. (Carlsbad, California, USA). The

AccuPower™ RT PreMix PCR kit, PPARγ, C/EBPα, and GAPDH oligonucleotide primers were purchased from Bioneer Co. (Daejeon, Korea). All other chemicals were purchased from Sigma Chemical Co. (St. Louis, MO, USA).

Preparation of E. splendens extracts

E. splendens was collected during the flowering season from September to October in Jeollanam-do, Korea. The plants were completely dried, separated into flowers, leaves, roots, and stems, and powdered. Powders (10 g) were extracted with 80 % ethanol under reflux for 2 h. Extracts were then evaporated at 50 °C using a rotary evaporator (Eyela, Tokyo, Japan), lyophilized using freeze-dryer (Ilshin, Seoul, Korea) to remove remaining solvent, diluted in 0.1 % DMSO (final concentration), and stored at 4 °C until required.

Total flavonoids and apigenin contents

Total flavonoid and apigenin contents within *E. splendens* ethanolic extracts were analyzed as previously reported (*21*). HPLC was performed using an Agilent 1100 system (Santa Clara, CA, USA) equipped with a quadrupole mass spectrometer. The HPLC method used for the qualitative and quantitative analysis of apigenin is shown in Table S1. The concentration of apigenin contained in the extract was calculated using an apigenin calibration curve.

Radical scavenging ability

To measure the radical scavenging ability, a 2,2-diphenyl-1-picrylhydrazyl (DPPH) assay was performed (*21*). The sample and 0.2 mM DPPH solution were mixed equally and incubated for 30 min at room temperature. Absorbance was read at 517 nm using a microplate reader (SYNERGY HTX, Biotek, CA, USA), and radical scavenging activity (in %) was calculated as:

$$\text{Radical scavenging ability} = (1 - (A(\text{sample})/A(\text{blank})) \cdot 100 \quad /1/$$

Evaluation of the in vitro effects of E. splendens extracts on adipocytes

Cell culture and adipocyte differentiation

3T3-L1 cells (from American Type Culture Collection (ATCC)) were cultured in 24-well plates (3×10^5 cells/well) and differentiated with or without extracts. Two days post-confluence (day 1), cells were exposed to induction medium (DMEM with 10 % FBS, 10 μg/mL insulin, 0.5 μM dexamethasone, and 0.5 mM isobutylmethylxanthine (IBMX). Differentiation was generally complete by day 8. Extracts (10–100 μg/mL) were added on day 0, 2, or 4 during differentiation, and cells were incubated until day 8 to reach the mature adipocyte stage.

MTT assay

Cell viability was assessed using a 3-(4,5-dimethylthiazol-2-yl)-2,5-diphenyl-tetrazolium bromide (MTT) assay (*5*). Cells were seeded on 96-well plates at a density of $1 \cdot 10^4$ cells per well, and 48 h after treatment, incubated with 1 mg/mL MTT for 1 h. The MTT solution was then removed, and the formazan produced was dissolved with DMSO. Cell viability was measured by spectrophotometry at 570 nm using a microplate reader (SYNERGY HTX, Biotek, CA, USA).

Cell proliferation assay

Cell proliferation was assessed by bromodeoxyuridine (BrdU)/propidium iodide (PI) immunofluorescence staining (*5*). Briefly, cells were seeded on glass coverslips in 3.5 cm dishes and differentiated as described. Cells were incubated with BrdU for 15 h, washed with PBS. They were then fixed and incubated with primary anti-BrdU monoclonal antibodies in 10 % NGS for 12 h at 4 °C, and then for 1 h with fluorescein isothiocyanate (FITC)-labeled secondary antibody and PI. Coverslips were washed with PBT, treated with PI solution (in PBS) for 30 min, mounted on slides, and observed under a fluorescence microscope (Nikon, Eclipse Ci-L, Seoul, Korea).

Oil Red O staining of adipocytes

3T3-L1 preadipocytes were induced to differentiate into mature adipocytes for 8 days, and then lipid accumulation was evaluated by Oil Red O (ORO) staining (*5*). Briefly, sample-treated cells were washed with PBS twice, fixed in 3.7 % paraformaldehyde, washed with 60 % isopropanol twice, and then stained with ORO solution for 1 h at room temperature. To quantify ORO uptake, cells were incubated with isopropanol, and the absorbance of red stained lipids was determined at 510 nm using a microplate reader (SYNERGY HTX, Biotek, CA, USA).

TG contents of adipocytes

To analyze intracellular TG contents, 3T3-L1 preadipocytes were washed twice with PBS and then scraped in 100 µL of lysis buffer (1 mM EDTA in 20 mM Tris). To measure TG contents, lysates were reacted with TG assay reagent, according to the manufacturer's instructions (Biomax, Guri-si, Gyeonggi-do, Republic of Korea) (*12*). Results are expressed as µg TG per ug cellular protein.

mRNA analysis

Total RNA was isolated from adipocytes with Trizol reagent and 1 µg was reverse-transcribed using RT Pre-mix. Quantitative PCR was performed using an MJ Mini Gradient Thermal Cycler (Bio-Rad, CA, USA). The used primer sequences and PCR analysis conditions are provided in Table S2

and Table S3, respectively. PCR products were fractionated on 2 % agarose gels in 0.5X TBE buffer and stained with ethidium bromide. Bands were visualized on a UV illuminator and recorded using an EL LoGic 100 Imaging System (Kodak, Tokyo, Japan). Image analysis was conducted using Quantity One software (Bio-Rad, CA, USA). GAPDH was used as an internal control to calculate the sample mRNA abundance. The band intensities were quantified using Image J (*22*).

Evaluation of the in vivo effects of ESFEs using C.elegans

C. elegans cultivation

C. elegans (N2, wild type), TJ356 DAF-16::GFP (zls356) IV, and *Escherichia coli* OP50 were obtained from the Caenorhabditis Genetics Center (CGC, MN, USA). Worms were cultured on nematode growth medium (NGM) plates at 20 °C. Torsos of mature worms were dissolved using 6 % house bleach, and residues were washed multiple times with M9 buffer to collect embryos for the preparation of synchronized worms. To evaluate the effect of the extract in a metabolic disease model of obesity, we fed the nematodes a 2 % glucose (GLU) diet for the duration of their growth.

Oil Red O staining of *C. elegans*

To quantify lipid accumulation in *C. elegans*, ORO staining was performed (*8*). L4 stage worms were treated with ESFE (25, 50, or 100 μg/mL) or apigenin (10, 20, or 40 μM) for 12 h. Young adult worms were grown in liquid media containing ESFE or apigenin, washed three times with PBS, fixed with 3.7 % paraformaldehyde for 10 min, and dehydrated with 60 % isopropanol for 5 min. Fixed worms were placed in ORO working solution for 2 h and washed with PBS. For imaging, approximately 20 worms were randomly selected under a Leica microscope equipped with DIC optics (Leica, Wetzlar, Germany) under identical settings and exposure times. ORO intensities were quantified using Image J (*22*).

TG contents of *C. elegans*

To quantify TG levels in worms, worms were washed twice with PBS and dissolved in 500 μL PBS including 0.05 % Tween 20, followed by homogenization on ice for 5 min. Ground samples were then centrifuged at 8,000 rpm for 5 min, and supernatants were used for measurements. TG levels were quantified using a free glycerol reagent, following the same kit and protocol as described for 3T3-L1 cells (*12*). Results are expressed as TG (μg) per cellular protein (mg).

Reactive oxygen species (ROS) intensity in *C. elegans*

L2 worms were exposed to different concentrations of ESFE and apigenin for 50 h, followed by staining with 100 μM H_2DCF-DA in the dark for 1 h. Worms were then mounted on slides with 2 % NaN_3 and observed using a fluorescence microscope (Nikon, Eclipse Ci-L, Seoul, Korea). Fluorescence intensity was analyzed using Image J, with approximately 15 worms per group used for quantification. This method was adapted with modifications from Kim *et al.* (*12*).

Nuclear translocation of DAF-16 in *C. elegans*

The DAF-16::GFP (zIs356) nematode is a transgenic mutant in which a green fluorescent protein is tagged to daf-16. We observed nuclear translocation of DAF-16 in adult nematodes after treatment with ESFE or apigenin for 50 hours from L2 stage. Nematodes were fixed with 2 % NaN_3 on slide glasses and observed under a fluorescence microscope (Nikon, Eclipse Ci-L, Seoul, Korea). DAF-16::GFP expression patterns were classified as “cytoplasmic,” “intermediate,” and “nuclear,” based on definitions from a previous study (*12*), to calculate the proportion of each group.

Statistical analysis

Results were presented as the mean value±S.D. of three independent experiments. ANOVA or Student *t*-test in SPSS v. 19.0 (*23*) were used to determine the statistical differences. Significance was accepted for $p<0.05$ or $p<0.01$ as determined by the *t*-test.

RESULTS AND DISCUSSION

Total flavonoid and apigenin contents of E. splendens extracts

In previous studies, the flavonoid content varied greatly depending on the origin, cultivation environment, plant part, and processing conditions of *E. splendens* (*19,29,30*). Therefore, qualitative and quantitative analysis of the active compounds needed to be prioritized before bioactivity evaluation. Previous studies have reported apigenin, quercetin, and rutin in ESFE (*19*), so we confirmed the content of these NaN_3 components in this study.

To assess the potential of the different parts of *E. splendens*, we examined the apigenin contents of roots, stems, leaves, and flowers. The total flavonoid and apigenin contents of plant flowers, leaves, roots, and stems are provided in Fig. 1. Apigenin was the predominant active compound of *E. splendens* (Fig. 1a). Both total flavonoid and apigenin contents were in decreasing order: flowers>leaves>roots>stems (Fig. 1b). The flower parts contained the highest levels of flavonoids and apigenin. In particular, apigenin was found to be abundant in the flowers, accounting for 66.28 % of the total flavonoids. These results are similar to previous findings by Um and Kim (*19*).

Effect of E. splendens extracts on 3T3-L1 cell viability

An MTT assay was used to examine the effects of *E. splendens* extracts on the viability of 3T3-L1 preadipocytes at extract levels of 25–100 μg/mL, which were equivalent to 17–68 μM of apigenin. No extract had a significant effect on the morphology or viability of confluent preadipocyte 3T3-L1 cells at concentrations of 25 or 50 μg/mL for 48 h. However, treatment with leaf and root extracts at 100 μg/mL significantly reduced cell viability (Fig. 2). The secondary metabolites contained in different parts of a plant may vary, which may result in differing efficacy and toxicity profiles. These variations highlight the importance of considering the specific plant part used in the development of plant-based products (*31*). The flower extract (hereafter ESFE) was considered to have the greatest potential among the four parts due to its high apigenin content and non-toxicity and was used for further *in vitro* and *in vivo* investigations.

Effects of ESFE and apigenin on 3T3-L1 cells differentiation and proliferation during adipogenesis

Adipose tissue formation involves two main processes: the proliferation of preadipocytes and their differentiation into mature adipocytes (*32*). Recently, various studies have shown that obesity might be prevented by adipocyte apoptosis and by inhibiting adipogenesis (*33,34*).

ESFE-treated cells prominently exhibited the dose-dependent inhibition of lipid accumulation in the cytoplasm compared to the MDI-treated cells (Fig. 3a and Fig. 3b). In particular, ESFE at 100 μg/mL resulted in a 50 % decrease in lipid accumulation compared to MDI-treated cells. Also, to further investigate the effect of ESFE on adipogenesis, cellular TG contents in adipocytes were measured. ESFE (100 μg/mL) significantly decreased intracellular TG contents to (57.60±0.88) μg/μg protein ($p<0.01$), compared to MDI-treated cells ((82.03±1.71) μg/μg protein) (Fig. 3c).

To determine the effect of ESFE on cell proliferation of preadipocytes, we performed a BrdU/PI assay on day 8 of differentiation. As shown in Fig. 3d, ESFE significantly inhibited proliferation.

The expression of mRNA of PPARγ and C/EBPα with or without ESFE (10–100 μg/mL) in MDI treated cells was measured by qPCR. In cells treated with ESFE (100 μg/mL), the expression of PPARγ and C/EBPα mRNA was reduced by 30 and 55 % ($p<0.01$), respectively, compared to cells treated with MDI control (Fig. 3e and Fig. 3f).

It was necessary to confirm whether the efficacy of ESFE was due to the apigenin that ESFE primarily contained. To evaluate its effect on cell viability, apigenin was administered to 3T3-L1 cells at 10–50 μM for 48 h. Cell viability at 50 μM decreased after 48 h, and therefore, we used concentrations in the range 10-40 μM in further tests (Fig. 4a).

Apigenin inhibited lipid and TG accumulation during adipogenesis (Fig. 4b, Fig. 4c and Fig. 4d). In particular, apigenin at 40 μM reduced lipid and TG contents by 92 and 80 %, respectively, during adipogenesis, which confirmed that the anti-adipogenic effect of ESFE on adipogenesis was caused by apigenin.

Taken together, ESFE has been shown to inhibit lipid accumulation by regulating both proliferation and the differentiation processes during adipogenesis of 3T3-L1 cells. In addition, during adipogenesis, ESFE was found to inhibit the increased expression of PPARγ and C/EBPα transcription factors associated with differentiation. These results suggest that the effects of ESFE might be due to apigenin. Previous studies have demonstrated that apigenin inhibits lipid accumulation by lowering the expression of PPARγ and C/EBPα during the differentiation of 3T3-L1 cells (*35,36*). Their work strongly supports our conclusion.

Inhibitory effect of ESFE and apigenin on lipid and TG accumulation in C. elegans

We employed *C. elegans* as an experimental animal model to see whether the effects of ESFE could work not only in the cellular level but also *in vivo* system. This inhibitory effect of ESFEs on lipid accumulation has been confirmed not only at the cellular level but also in animal models. Because *C. elegans* has transparent torso, individual cells are easily visualized by staining (*37*). Thus, we were able to induce obesity in *C. elegans* with a high GLU diet and then observe the phenotypic and physiological responses.

As was observed for 3T3-L1 cells, lipid and TG accumulation decreased in ESFE and apigenin treatment groups (Fig. 5). When nematodes induced to become obese by a high GLU diet were exposed to ORO solution, it was observed that their deposited body fat stained red strongly, and the intensity of the red color was reduced when ESFE was consumed (Fig. 5a). In particular, apigenin at 40 μM significantly inhibited lipid and TG accumulations by 82 and 89 % compared to the control, respectively (Fig. 5b and Fig. 5c), which showed that the effects of ESFE and apigenin occur at the cellular level and in animal systems. Choi and Kim (*38*) reported *E. splendens* extracts dose-dependent decrease in blood TG and LDL in mice fed the extracts. Although they did not observe morphological changes in adipose tissue, they demonstrated that *E. splendens* extracts improved the lipid metabolism in mammals (*38*).

Effect of ESFE and apigenin on the nuclear translocation of DAF-16 in C. elegans

To assess whether ESFE and apigenin respond to DAF-16/FOXO under a high GLU diet, we used nematodes with a GFP-tagged DAF-16 protein and monitored the nuclear translocation of DAF-16. As a result, we observed an increase in the nuclear translocation of DAF-16 in dependence on

ESFE and apigenin concentration (Fig. 6). In other words, we have demonstrated that DAF-16 is involved in the metabolic stress caused by a high GLU diet and that ESFE and apigenin can modulate this metabolism.

DAF-16/FOXOs are associated with insulin resistance and regulate energy metabolism (*9,10*). FOXO1, particularly, is involved in cell cycle regulation during adipocyte differentiation and ultimately influences cell death or cell proliferation (*9-11*). FOXO1 also regulates adipocyte differentiation by modulating the expression of PPARγ (*9-11,39*). This study strongly suggests that ESFE relies on FOXO to inhibit lipid accumulation by: 1) regulating the cell cycle to inhibit preadipocyte proliferation and 2) regulating PPARγ to inhibit differentiation into adipocytes. Nevertheless, there are several limitations to this study. We did not identify a direct relationship between FOXO and cell proliferation or cell differentiation in either cell or nematode models in the molecular level. Therefore, further studies should elucidate the FOXO downstream molecular mechanism on the inhibitory effect of ESFE during adipogenesis in independent experimental models.

Effect of ESFE and apigenin on ROS accumulation in C. elegans

A previous study has investigated whether GLU induces oxidative stress and found that it does in a glucose concentration-dependent manner in nematodes (*12*). Therefore, we induced oxidative metabolic stress with 2 % GLU. Nematodes treated with ESFE and apigenin showed a concentration-dependent inhibition of ROS accumulation compared to the control (Fig. 7a and Fig. 7b). *In vitro* radical scavenging activity also showed that ESFE at 100 μg/mL and apigenin at 40 μM had similar effects as the control, 40 μM trolox (Fig. 7c). Several studies have reported that ESFE and apigenin possess antioxidant properties (*20,24,25*) and they support our findings. Meanwhile, numerous studies have demonstrated the interplay between reactive oxygen species (ROS) and fat accumulation in the context of metabolic diseases, with the involvement of DAF-16 (*8,40*). In addition, previous reports have shown that nuclear localization of DAF-16 is a prerequisite for the activation of Antioxidant-related genes including Mn-SOD (sod-3) and catalases (ctl-1 and ctl-2), which regulate ROS production (*12,41,42*). These have led to a novel hypothesis that ESFE might modulate FOXO translocation into the nucleus to reduce ROS, thereby ameliorating obesity and its complications, metabolic diseases. Indeed, in the present study, the intranuclear expression of daf-16 was increased and ROS was reduced by the antioxidant properties of ESFE and apigenin under oxidative stress conditions caused by high glucose intake in nematodes.

In obesity, enlarged fat cells lead to lipid metabolic imbalances and oxidative stress, resulting in excessive ROS production. ROS contribute to metabolic disorders, such as inflammation and insulin resistance, further exacerbating lipid imbalances and promoting obesity-related diseases (*13*).

Therefore, the inhibition of lipid accumulation and ROS production represents a dual challenge in the treatment of metabolic diseases, including obesity (*43*). A growing body of evidence has highlighted the therapeutic potential of antioxidants as adjuncts in obesity prevention and treatment, suggesting that their use may significantly improve overall health outcomes.

CONCLUSIONS

In conclusion, ESFE and its bioactive component, apigenin were found to lower lipid and TG levels in 3T3-L1 cells and *C. elegans*. The results obtained indicate that ESFE inhibits adipogenic differentiation, and that this inhibition was involved in the downregulation of PPARγ and C/EBPα at the molecular level. Furthermore, an increased intranuclear expression of DAF-16/FOXO was found in nematodes. Taken together, these results suggest that ESFE might inhibit adipose accumulation by increasing FOXO and inducing a decrease in the adipogenic factors PPARγ and C/EBPα. In addition, ESFE inhibited ROS overproduction. Therefore, ESFE-containing apigenin could be utilized as a material that exhibits positive effects against obesity-related metabolic stress. Previous research on *E. splendens* has mainly focused on the plant characteristics in relation to its cultivation and growth. Our findings provide new insights, as there is a dearth of research on the efficacy of *E. splendens* for metabolic diseases, including obesity. However, to advance the development of *E. splendens* as a functional food for health promotion, further studies are needed to investigate its molecular efficacy, particularly the activation of PPARγ and C/EBPα in relation to DAF-16 in mammalian models. Additionally, toxicity assessments and pharmacokinetic evaluations should be conducted to ensure its safety and effectiveness.

FUNDING

This research was supported by National Research Foundation of Korea (NRF), funded by the Korea government (MSIP) (Grant no. 2021R1G1A1092967).

CONFLICT OF INTEREST

The authors report no conflict of interest.

AUTHORS' CONTRIBUTION

SL conducted experiments, analysed data, and wrote the manuscript. SIC conducted experiments and analysed the data. MJ designed, analysed, and supervised the research and wrote the manuscript.

ORCID ID

S.B. Lee https://orcid.org/0009-0007-0261-9404

S.I. Choi https://orcid.org/0000-0002-8362-3523

M. Jang https://orcid.org/0000-0001-5934-982X

REFERENCES

1. Malik VS, Hu FB. The role of sugar-sweetened beverages in the global epidemics of obesity and chronic diseases. Nat Rev Endocrinol. 2022;18(4):205–18. https://doi.org/10.1038/s41574-021-00627-6

2. García-Sánchez A, Miranda-Díaz AG, Cardona-Muñoz EG. The role of oxidative stress in physiopathology and pharmacological treatment with pro- and anti-oxidant properties in chronic diseases. Oxid Med Cell Longev. 2020;2020:e2082145. https://doi.org/10.1155/2020/2082145

3. Zhu S, Wang W, Zhang J, Ji S, Jing Z, Chen YQ. Slc25a5 regulates adipogenesis by modulating ERK signaling in OP9 cells. Cell Mol Biol Lett. 2022;27(1):11. https://doi.org/10.1186/s11658-022-00314-y

4. Zuo Y, Qiang L, Farmer SR. Activation of CCAAT/enhancer-binding protein (C/EBP) α expression by C/EBPβ during adipogenesis requires a peroxisome proliferator-activated receptor-γ-associated re-pression of HDAC1 at the C/EBPα gene promoter. J Biol Chem. 2006;281(12):7960–7. https://doi.org/10.1074/jbc.M510682200

5. Jang M, Choi S. Schisandrin C isolated from *Schisandra chinensis* fruits inhibits lipid accumulation by regulating adipogenesis and lipolysis through AMPK signaling in 3T3-L1 adipocytes. J Food Biochem. 2022;46(12):e14454. https://doi.org/10.1111/jfbc.14454

6. Kinser HE, Pincus Z. High-throughput screening in the *C. elegans* nervous system. Mol Cell Neurosci. 2017;80:192–7. https://doi.org/10.1016/j.mcn.2016.06.001

7. Jang M, Kim KH, Kim GH. Antioxidant capacity of thistle (*Cirsium japonicum*) in various drying methods and their protection effect on neuronal PC12 cells and *Caenorhabditis elegans*. Antioxidants. 2020;9(3):200. https://doi.org/10.3390/antiox9030200

8. Kim Y, Nam S, Lim J, Jang M. Autumn olive (*Elaeagnus umbellata* Thunb.) berries improve lipid metabolism and delay aging in middle-aged *Caenorhabditis elegans.* Int J Mol Sci. 2024;25(6):e3418.
https://doi.org/10.3390/ijms25063418
9. Chen J, Lu Y, Tian M, Huang Q. Molecular mechanisms of FOXO1 in adipocyte differentiation. J Mol Endocrinol. 2019;62(3):R239–53.
https://doi.org/10.1530/JME-18-0178
10. Boughanem H, Cabrera-Mulero A, Millán-Gómez M, Garrido-Sánchez L, Cardona F, Tinahones FJ, Moreno-Santos I, Macías-González M. Transcriptional analysis of FOXO1, C/EBP-α and PPAR-γ2 genes and their association with obesity-related insulin resistance. Genes. 2019;10(9):706.
https://doi.org/10.3390/genes10090706
11. Nakae J, Kitamura T, Kitamura Y, Biggs III WH, Arden KC, Accili D. The Forkhead transcription factor Foxo1 regulates adipocyte differentiation. Dev Cell. 2003;4(1):119–29.
https://doi.org/10.1016/S1534-5807(02)00401-X
12. Kim Y, Lee SB, Cho M, Choe S, Jang M. Indian almond (*Terminalia catappa* Linn.) leaf extract extends lifespan by improving lipid metabolism and antioxidant activity dependent on AMPK signaling pathway in *Caenorhabditis elegans* under high-glucose-diet. Antioxidants 2024;13(1):14.
https://doi.org/10.3390/antiox13010014
13. Manna P, Jain SK. Obesity, oxidative stress, adipose tissue dysfunction, and the associated health risks: Causes and therapeutic strategies. Metab Syndr Relat Disord. 2015;13(10):423–44.
https://doi.org/10.1089/met.2015.0095
14. Cho M, Park H, Lee SH, Kim MJ, Jang M. Phyllodulcin from the hexane fraction of *Hydrangea macrophylla* inhibits glucose-induced lipid accumulation and reactive oxygen species generation in *Caenorhabditis elegans*. Biosci Biotechnol Biochem. 2024;88(7):789-97.
https://doi.org/10.1093/bbb/zbae043
15. Jang M, Choi HY, Kim GH. Phenolic components rich ethyl acetate fraction of *Orostachys japonicus* inhibits lipid accumulation by regulating reactive oxygen species generation in adipogenesis. J Food Biochem. 2019;43(8):e12939.
https://doi.org/10.1111/jfbc.12939
16. Jang M, Choi HY, Kim GH. Inhibitory effects of *Orostachys malacophyllus* var. iwarenge extracts on reactive oxygen species production and lipid accumulation during 3T3-L1 adipocyte differentiation. Food Sci Biotechnol 2019; 28:227–36.
https://doi.org/10.1007/s10068-018-0426-x

17. Choi HS, Min KC. Aroma-active compounds of *Elsholtzia splendens* using AEDA and HS–SPME–GC–O dilution analysis. Flavour Fragr J. 2008;23(1):58–64. https://doi.org/10.1002/ffj.1856

18. Song, S.E.; Chae, Y.A. Characteristics of volatile oil components in *Elsholtzia splendens* Nakai collected in Korea. Korean J Med Crop Sci 2004;12(6):459–62.

19. Lee SY, Chung MS, Kim MK, Baek HH, Lee MS. Volatile compounds of *Elsholtzia splendens*. Korean J Food Sci Technol. 2005;37(3):339–44.

20. Lee JS, Kim GH, Lee HG. Characteristics and antioxidant activity of *Elsholtzia splendens* extract-loaded nanoparticles. J Agric Food Chem 2010;58(6):3316–21. https://doi.org/10.1021/jf904091d

21. Um HJ, Kim GH. Studies on the flavonoid compositions of *Elsholtzia* spp. Korean J Food Nutr 2007;20(2):103–7.

22. Schneider CA, Rasband WS, Eliceiri KW. NIH Image to ImageJ: 25 years of image analysis. Nat Methods. 2012;9:671–5. https://doi.org/10.1038/nmeth.2089

23. IBM SPSS Statistics for Windows, v. 30.0. IBM Corp., Armonk, NY, USA; 2019. Available from: https://www.ibm.com/products/spss-statistics.

24. Guo Z, Liu Z, Wang X, Liu W, Jiang R, Cheng R, She G. *Elsholtzia*: phytochemistry and biological activities. Chem Cent J. 2012;6(1):1–8. https://doi.org/10.1186/1752-153X-6-147

25. Choi EJ, Lee YS, Kim GH. Antioxidative characteristics of extracts from aromatic herb *Elsholtzia splendens*. Food Sci Biotechnol. 2007;16(3):489–92.

26. Kim DW, Son KH, Chang HW, Bae K, Kang SS, Kim HP. Anti-inflammatory activity of *Elsholtzia splendens*. Arch Pharm Res. 2003;26(3):232–6. https://doi.org/10.1007/BF02976835

27. Ali F, Rahul Naz F, Jyoti S, Siddique YH. Health functionality of apigenin: A review. Int J Food Prop. 2017;20(6):1197–238. https://doi.org/10.1080/10942912.2016.1207188

28. Zhou X, Wang F, Zhou R, Song X, Xie M. Apigenin: A current review on its beneficial biological activities. J Food Biochem. 2017;41(4):e12376. https://doi.org/10.1111/jfbc.12376

29. Lee JS, Kim GH, Lee HG. Optimization of extraction conditions for *Elsholtzia splendens* and its antioxidant activity. J Food Biochem. 2013;37(6):669–76.

https://doi.org/10.1111/j.1745-4514.2012.00662.x

30. Yossa Nzeuwa IB, Guo B, Zhang T, Wang L, Ji Q, Xia H, Sun G. Comparative metabolic profiling of *Lycium* fruits (*Lycium barbarum* and *Lycium chinense*) from different areas in China and from Nepal. J Food Qual. 2019;2019:1–6.
https://doi.org/10.1155/2019/4396027

31. Deka B, Manna P, Borah JC, Talukdar NC. A review on phytochemical, pharmacological attributes and therapeutic uses of *Allium hookeri*. Phytomed Plus. 2022;2(2):e100262.
https://doi.org/10.1016/j.phyplu.2022.100262

32. Jasaszwili M, Wojciechowicz T, Billert M, Strowski MZ, Nowak KW, Skrzypski M. Effects of adropin on proliferation and differentiation of 3T3-L1 cells and rat primary preadipocytes. Mol Cell Endocrinol. 2019;496(1):e110532.
https://doi.org/10.1016/j.mce.2019.110532

33. Lin J, Della-Fera MA, Baile CA. Green tea polyphenol epigallocatechin gallate inhibits adipogenesis and induces apoptosis in 3T3-L1 adipocytes. Obesity Res. 2005;13(6):982–90.
https://doi.org/10.1038/oby.2005.115

34. Rayalama S, Della-Feraa MA, Bailea CA. Phytochemicals and regulation of the adipocyte life cycle. J Nutr Biochem. 2008;19(11):717–26.
https://doi.org/10.1016/j.jnutbio.2007.12.007

35. Ono M, Fujimori K. Antiadipogenic effect of dietary apigenin through activation of AMPK in 3T3-L1 cells. J Agric Food Chem. 2011;59(24):13346–52.
https://doi.org/10.1021/jf203490a

36. Kim MK, Kang K, Lee HJ, Kim M, Kim CY, Nho CW. Apigenin isolated from *Daphne genkwa* Siebold et Zucc. inhibits 3T3-L1 preadipocyte differentiation through a modulation of mitotic clonal expansion. Life Sci. 2014;101(1–2):64–72.
https://doi.org/10.1016/j.lfs.2014.02.012

37. Shen P, Yue Y, Park Y. A living model for obesity and aging research: *Caenorhabditis elegans*. Crit Rev Food Sci Nutr. 2018;58(5):741–54.
https://doi.org/10.1080/10408398.2016.1220914

38. Choi EJ, Kim GH. Effect of *Elsholtzia splendens* extracts on the blood lipid profile and hepatotoxicity of the mice. Food Sci Biotechnol. 2008;17(2):413–6.

39. Dowell P, Otto TC, Adi S, Lane MD. Convergence of peroxisome proliferator-activated receptor γ and Foxo1 signaling pathways. J Biol Chem. 2003;278(46):45485–91.
https://doi.org/10.1074/jbc.M309069200

40. Wang K, Chen S, Zhang C, Huang J, Wu J, Zhou H, Jin L, Qian X, Jin J, Lyu, J. Enhanced ROS production leads to excessive fat accumulation through DAF-16 in *Caenorhabditis elegans*. Exp Gerontol. 2018;112(2):20–9.
https://doi.org/10.1016/j.exger.2018.07.017

41. Park S, Park SK. Antioxidant and anti-aging effects of phlorizin are mediated by DAF-16-induced stress response and autophagy in *Caenorhabditis elegans*. Antioxidants. 2022;11(10):1996.
https://doi.org/10.3390/antiox11101996

42. Li WH, Shi YC, Chang CH, Huang CW, Liao VH. Selenite protects *Caenorhabditis elegans* from oxidative stress via DAF-16 and TRXR-1. Mol Nutr Food Res. 2014;58(4):863–74.
https://doi.org/10.1002/mnfr.201300404

43. Sood P, Kaur G, Thapa K, Sharma K, Sindhu RK. Antioxidants and obesity. In: Sindhu RK, Singh I, Babu MA, editors. Antioxidants: Nature's defense against disease. Oxford, UK: Wiley-Blackwell; 2024. pp. 491-510.
https://doi.org/10.1002/9781394270576.ch13

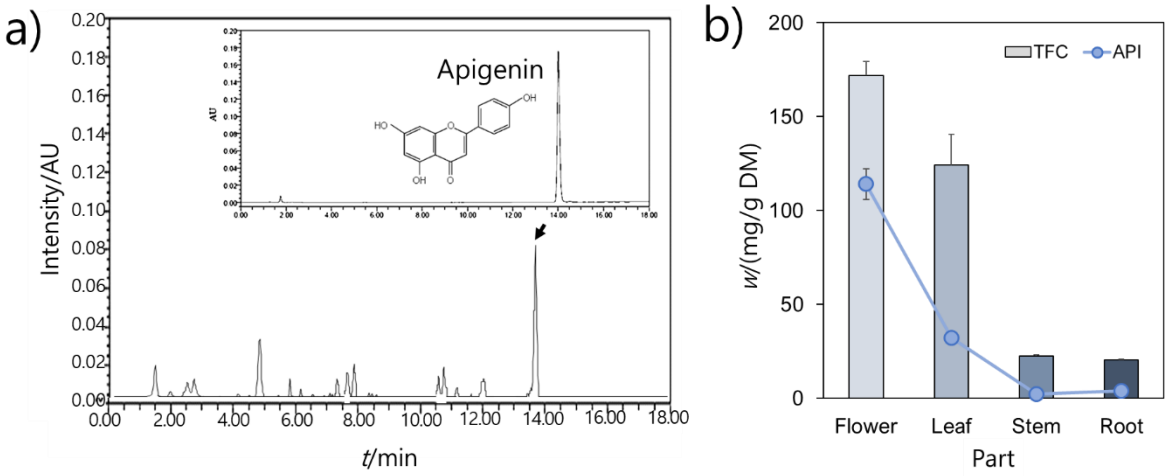

Fig. 1. Total flavonoid and apigenin contents of the various parts of *E. splendens*. a) HPLC Chromatogram of *E. splendens* flower extract (ESFE) and apigenin. b) The total flavonoid and

apigenin contents of various parts of *E. splendens*. Results are shown as the mean±SD of three independent experimental values

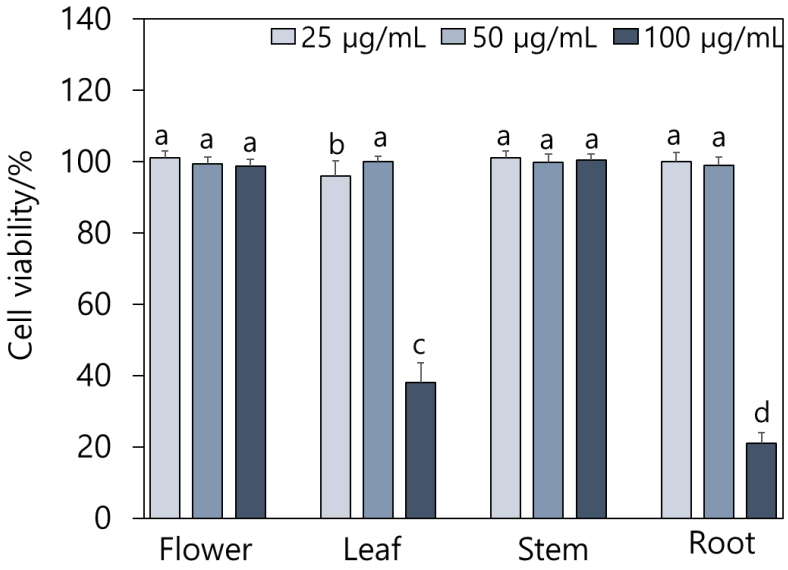

Fig. 2. Effect of *E. splendens* extracts on 3T3-L1 cell viability. 3T3-L1 preadipocytes were exposed to different parts of *E. splendens* extract (25, 50 and 100 μg/mL) for 48 h. Cell viabilities were measured using an MTT assay. Results are shown as the mean value±S.D. of three independent experimental values. Letters (a-d) indicate significant differences at $p<0.05$

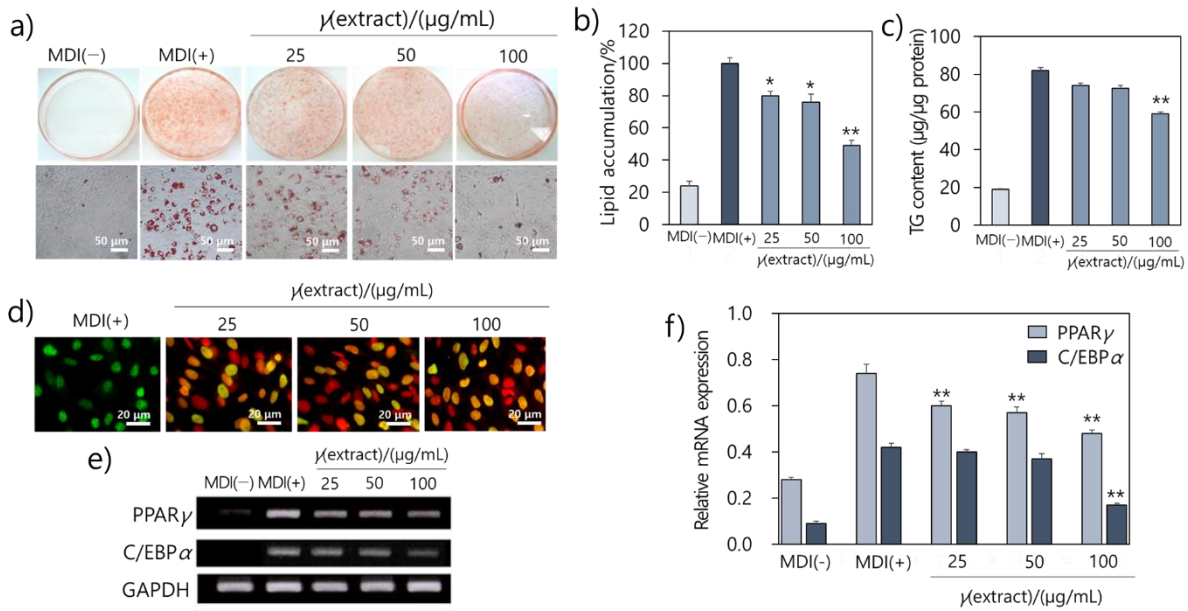

Fig. 3. Effect of ESFE on cell proliferation and lipid accumulation during adipogenesis. Cells were differentiated into adipocytes for 8 days in medium with or without ESFE (25, 50, and 100 μg/mL). a) Image of lipid droplets of ORO-stained adipocytes, b) total lipid contents of ESFE-treated adipocytes, c) intracellular TG contents of ESFE-treated adipocytes, d) cell proliferation investigated by BrdU immunostaining, e) bands indicate expressed PPAR-γ, C/EBPα, and GAPDH mRNAs, and f) bar graph showing PPAR-γ/GAPDH and C/EBPα/GAPDH ratios. Results are shown as the mean value±S.D. of three independent experimental values. The significance of differences between MDI control and ESFE-treated 3T3-L1 cells are indicated by *p<0.05 or **p<0.01

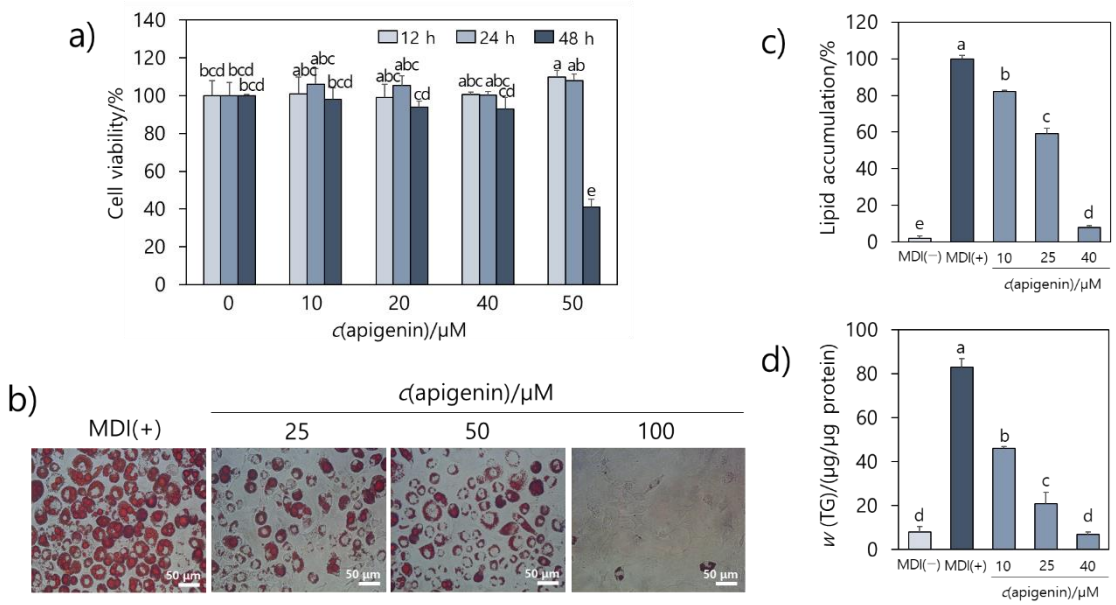

Fig. 4. Effect of apigenin on lipid accumulation during adipogenesis. Cells were differentiated into adipocytes for 8 days in medium with or without apigenin (10, 20, and 40 μM). a) Apigenin effects on 3T3-L1 cell viability measured by MTT assay, b) image of lipid droplets of ORO-stained adipocytes, c) total lipid contents of apigenin-treated adipocytes, d) intracellular TG contents of apigenin-treated adipocytes. Results are shown as the mean value±S.D. of three independent experimental values. Letters (a-e) indicate significant differences at $p<0.05$

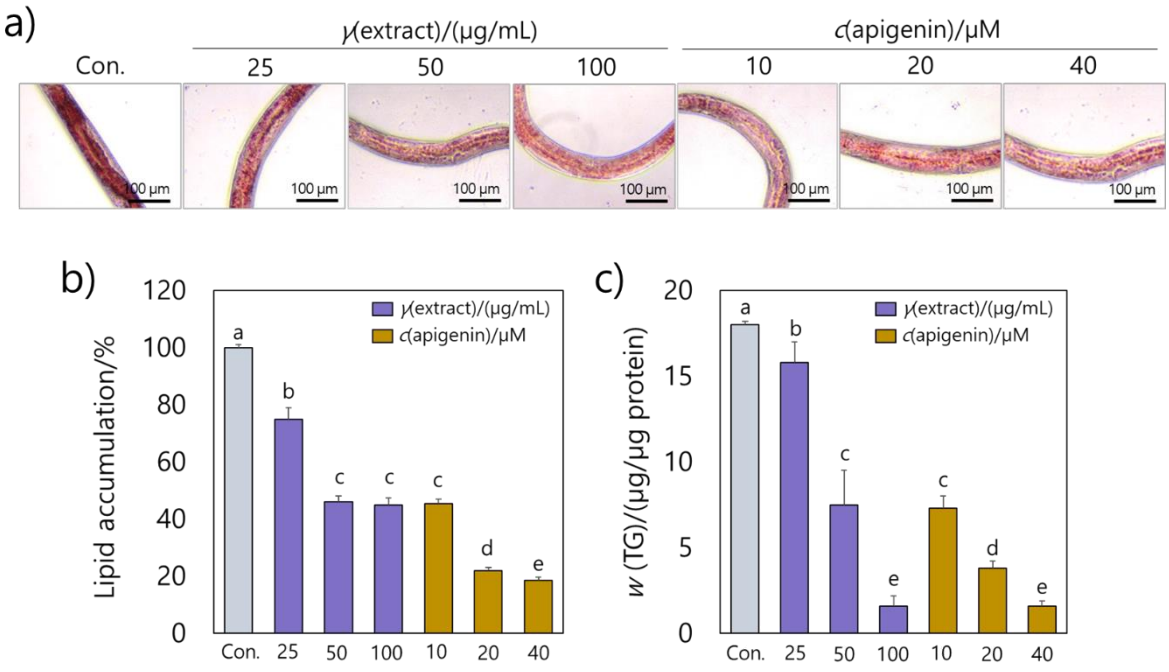

Fig. 5. The inhibitory effect of ESFE and apigenin on lipid accumulation in *C. elegans*. L4 stage worms were treated with ESFE (25, 50, or 100 μg/mL) or apigenin (10, 20, or 40 μM) for 12 h. a) Images of ORO-stained lipid droplets of *C. elegans*, b) total lipid contents of ESFE- or apigenin-treated apigenin-treated *C. elegans*, and c) TG contents of ESFE- or apigenin-treated apigenin-treated *C. elegans.* Results are shown as the mean value±S.D. of three independent experimental values ($N \geq 20$). Letters (a-e) indicate significant differences at $p<0.05$

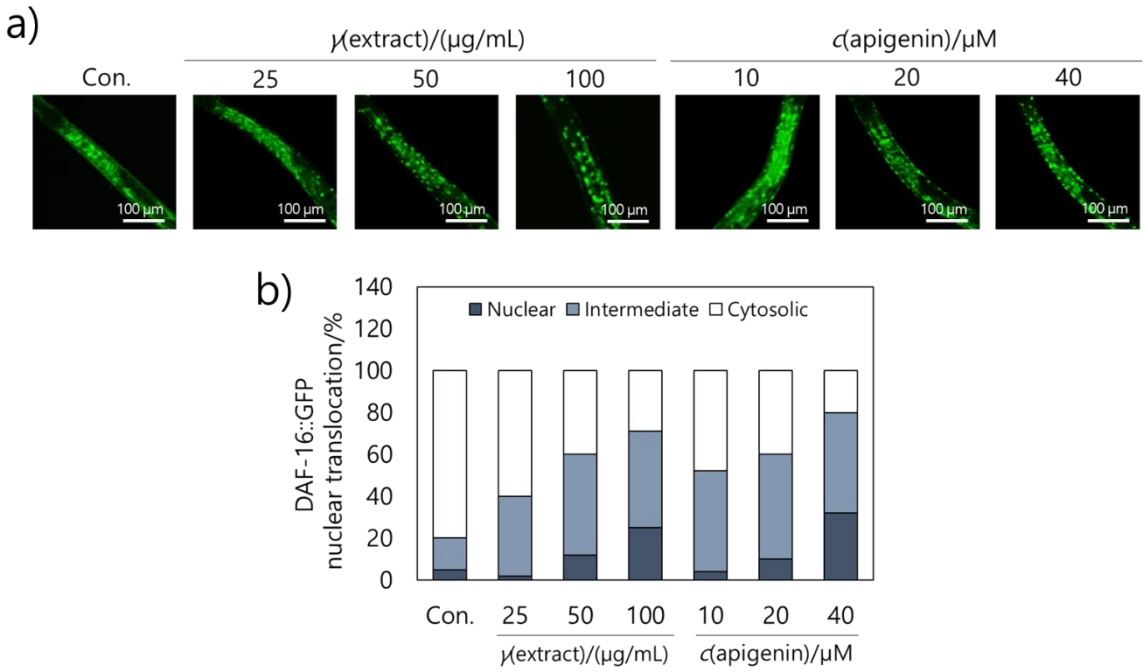

Fig. 6. ESFE and apigenin induced the nuclear translocation of DAF-16 in *C. elegans*. Nematodes were treated with ESFE (25, 50, or 100 μg/mL) or apigenin (10, 20, or 40 μM) for 72 h, then observed for the DAF-16::GFP-localization phenotype. a) Representative images of the transgenic strain TJ356 worm showing cytosolic, intermediate, and nuclear DAF-16 localization. b) Activation of DAF-16 nuclear translocation by ESFE and apigenin. Results are shown as the mean value±S.D. of three independent experimental values ($N \geq 20$)

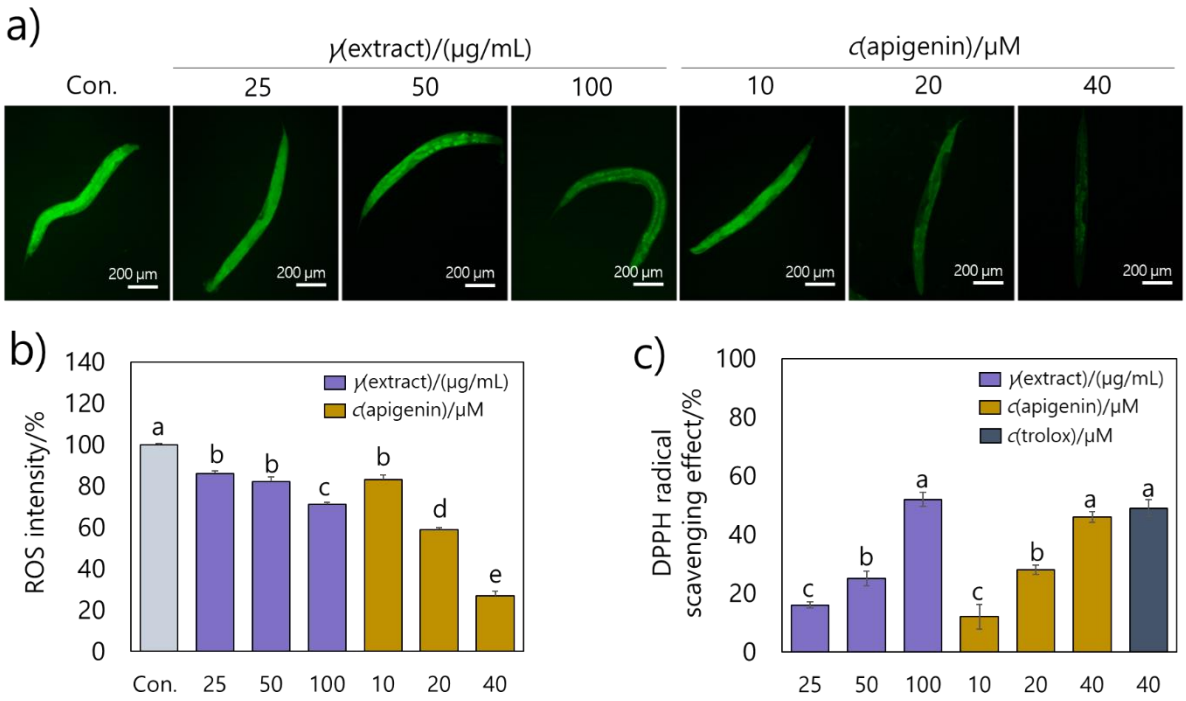

Fig. 7. Effect of ESFE and apigenin on ROS inhibition in *C. elegans*. L2 stage worms were treated with ESFE (25, 50, or 100 μg/mL) or apigenin (10, 20, or 40 μM) for 50 h. a) Images of green-fluorescent ROS of *C. elegans*, b) quantitative ROS intensities of ESFE- or apigenin-treated *C. elegans* ($N \geq 20$), and c) DPPH radical scavenging activity of ESFE and apigenin. Results are shown as the mean value±S.D. of three independent experimental values. Letters (a-e) indicate significant differences at $p<0.05$

SUPPLEMENTARY MATERIAL

Table S1. HPLC operating conditions

HPLC model	Agilent 1100 system (Santa Clara, CA, USA)
Column	Capcell pak C18VG 120 (250 ×4.6 mm, 5 μm)
Mobile phase	A: 0.1% formic acid in water
	B: 0.1% formic acid in acetonitrile
Gradient	A: 80–45 % (B: 20–55 %) for 15 min
Detection wavelength	UV 345 nm
Flow rate	1.0 mL/min
Injection volume	10 μLmm

Table S2. Primer sequences used for PCR

Gene	Primer	Sequence
PPARγ	Forward	5'-ACC ACT CGC ATT CCT TTG AC-3'
	Reverse	5'-TCA GCG GGA AGG ACT TTA TG-3'
C/EBPα	Forward	5'-ATG GAG TCG GCC GAC TTC TAC-3'
	Reverse	5'-CAG GAA CTC GTC GTT GAA GGC-3'
GAPDH	Forward	5'-AAC TTT GGC ATT GTG GAA GGG C-3'
	Reverse	5'-GAC ACA TTG GGG GTA GGA ACA C-3'

Table S3. PCR operating conditions

Step	Temperature/°C	*t*/min	Cycle
Initial	95	3	1
Amplification	94	0.5	25
	55	0.5	
	72	1	
Final extension	72	5	1